



HAL
open science

Rational Synthesis and Characterization of the Mixed-Metal Organometallic Polyoxometalates $[\text{Cp}^*\text{Mo}_x\text{W}_{6-x}\text{O}_{18}] - (x = 0, 1, 5, 6)$

Gülnur Taban-Çalışkan, Daniel Mesquita Fernandes, Jean-Claude Daran, Dominique Agustin, Funda Demirhan, Rinaldo Poli

► **To cite this version:**

Gülnur Taban-Çalışkan, Daniel Mesquita Fernandes, Jean-Claude Daran, Dominique Agustin, Funda Demirhan, et al.. Rational Synthesis and Characterization of the Mixed-Metal Organometallic Polyoxometalates $[\text{Cp}^*\text{Mo}_x\text{W}_{6-x}\text{O}_{18}] - (x = 0, 1, 5, 6)$. *Inorganic Chemistry*, 2012, 51 (10), pp.5931-5940. 10.1021/ic300578g . hal-03156138

HAL Id: hal-03156138

<https://hal.science/hal-03156138>

Submitted on 2 Mar 2021

HAL is a multi-disciplinary open access archive for the deposit and dissemination of scientific research documents, whether they are published or not. The documents may come from teaching and research institutions in France or abroad, or from public or private research centers.

L'archive ouverte pluridisciplinaire **HAL**, est destinée au dépôt et à la diffusion de documents scientifiques de niveau recherche, publiés ou non, émanant des établissements d'enseignement et de recherche français ou étrangers, des laboratoires publics ou privés.

**Rational synthesis and characterization of the mixed-metal organometallic
polyoxometalates $[\text{Cp}^*\text{Mo}_x\text{W}_{6-x}\text{O}_{18}]^-$ ($x = 0, 1, 5, 6$)**

Gülnur Taban-Çalışkan,^[a,b,c,d] Daniel Mesquita Fernandes,^[a,b,c] Jean-Claude Daran,^[a,b]

Dominique Agustin,^{*[a,b,c]} Funda Demirhan,^{*[d]} and Rinaldo Poli^{*[a,b,e]}

[a] CNRS, LCC (Laboratoire de Chimie de Coordination), 205 route de Narbonne,
BP 44099, F-31077 Toulouse Cedex 4, France

Fax: (+) 33-561553003. E-mail: rinaldo.poli@lcc-toulouse.fr

[b] Université de Toulouse, UPS, INPT, F-31077 Toulouse Cedex 4, France

[c] Institut Universitaire de Technologie Paul Sabatier; Département de Chimie; Av.
Georges Pompidou, BP 20258, F-81104 Castres Cedex, France

Fax: (+) 33-563356388. E-mail: dominique.agustin@iut-tlse3.fr

[d] Celal Bayar University, Faculty of Sciences & Liberal Arts, Department of Chemistry,
45030 Muradiye-Manisa, Turkey

Fax: (+) 90-02362412158. E-mail: funda.demirhan@bayar.edu.tr

[e] Institut Universitaire de France, 103, bd Saint-Michel, 75005 Paris, France.

Keywords:

Organometallic oxides / tungsten / molybdenum / polyoxometalates / DFT calculation / X-ray
crystallography

Abstract

The reaction between of the oxometallic complexes $\text{Cp}^*_2\text{M}_2\text{O}_5$ and $\text{Na}_2\text{M}'\text{O}_4$ ($\text{M}, \text{M}' = \text{Mo}, \text{W}$) in a 1/10 molar ratio in an acidic aqueous medium constitutes a mild and selective entry into the anionic Lindqvist-type hexametallc organometallic mixed oxides $[\text{Cp}^*\text{Mo}_x\text{W}_{6-x}\text{O}_{18}]^-$ ($x = 6$ (**1**), 5 (**2**), 1 (**3**), 0 (**4**)). All these compounds have been isolated as salts of $n\text{Bu}_4\text{N}^+$ (**a**), $n\text{Bu}_4\text{P}^+$ (**b**), and Ph_4P^+ (**c**) cations and two of them (**1**, **3**) also with the *n*-butylpyridinium ($n\text{BuPyr}^+$, **d**) cation. The compounds have been characterized by elemental analyses, thermogravimetric analyses, electrospray mass spectrometry, and infrared spectroscopy. The molecular identity and geometry of compounds **1c**, **2a** and **2c** has been confirmed by single crystal X-ray diffraction. DFT calculations on models obtained by replacing Cp^* with Cp (**I-IV**) have provided information on the assignment of the terminal $\text{M}=\text{O}$ and bridging $\text{M}-\text{O}-\text{M}$ vibrations.

Introduction

Materials based on mixed oxides are interesting for heterogeneous catalysis¹⁻⁷ as well as for chromogenic materials.⁸ Their properties (reactivity, light absorption, ...) may be fine tuned by subtle modification of the nature and relative proportion of the different metals. Fine control of the composition and homogeneity of these materials, however, can only be partially achieved by the current techniques (sputtering, CVD), since it is difficult to control a mixed and homogeneous metal distribution at the atomic level.⁹ In order to facilitate this task, the use of single source precursors is being sought but this strategy, often making use of mixed-metal alkoxides, needs strictly controlled environments (inert atmosphere, reduced pressure), since the precursors suffer from hydrolytic sensitivity.¹⁰⁻¹⁸

Polyoxometalates (POMs), in addition to being interesting molecular compounds in their own right,¹⁹ may also be considered as “molecular scale” models of metal oxides and are useful for the understanding the interaction of substrates and oxide surfaces in heterogeneous oxidation catalysis.²⁰⁻²² POMs are interesting compounds due their numerous potential applications especially in materials science and catalysis.²³ Although the elemental composition and morphological constitution of POMs can be precisely controlled,^{23,24} the synthesis of well defined heterometallic POMs often suffers from serendipity and results in a random distribution of the different metals in the structure. Rational strategies that have been employed to prepare heterometallic POMs are (i) the assembly of predefined polyatomic fragments sometimes performed in organic solvents and with air- and water-sensitive organometallic precursors and (ii) the grafting of simple organic fragments on lacunary oxoclusters.²⁵⁻³⁴ The use of hydrothermal methods starting from elementary bricks is another alternative strategy, the outcome of which is however largely affected by serendipity.^{31,35} POMs grafted with organometallic fragment have attracted interest³⁶⁻⁴² because the

organometallic fragment may impart a different reactivity to the molecule with respect to the all-inorganic POMs, obtaining mixed-metal clusters under mild conditions (often using aqueous solutions). As illustrative examples, the reaction of Na_2MO_4 ($\text{M} = \text{Mo}, \text{W}$) with $[\text{Cp}^*\text{RhCl}_2]_2$ or $[(\eta^6\text{-arene})\text{RuCl}_2]_2$ in water or acetonitrile yielded the octanuclear compounds $[(\text{LM})(\text{M}'\text{O})(\mu\text{-O})_3]_4$ [$\text{LM} = \text{Cp}^*\text{Rh}$ and $(p\text{-MeC}_4\text{H}_4i\text{Pr})\text{Ru}$ for $\text{M}' = \text{Mo}$;^{36,37,40} $\text{LM} = (\text{C}_6\text{Me}_6)\text{Ru}$ and $(p\text{-MeC}_4\text{H}_4i\text{Pr})$ for $\text{M}' = \text{W}$].⁴²

Recently, we have reported the use of $\text{Cp}^*_2\text{M}_2\text{O}_5$ ($\text{M} = \text{Mo}, \text{W}$), compounds that are stable in air and in aqueous solution in the entire pH range,⁴³ in combination with the inorganic salts $\text{Na}_2\text{M}'\text{O}_4$ ($\text{M}' = \text{Mo}, \text{W}$) in a 1:4 ratio, as precursors of the hexanuclear organometallic polyoxometallic complexes $\text{Cp}^*_2\text{Mo}_x\text{W}_{6-x}\text{O}_{17}$ ($x = 0, 2, 4, 6$) in a selective, high-yielding, room temperature aqueous reaction.^{44,45} The formula of these compounds may also be written as $[(\text{Cp}^*\text{M})_2(\text{M}'\text{O})_4(\mu_2\text{-O})_{12}(\mu_6\text{-O})]$. The relative position of the M and M' atoms is perfectly defined by the nature of the starting materials, the M element from the organometallic reagent ending up selectively in the (Cp^*M) positions and the M' element from the inorganic reagent occupying selectively the $(\text{M}'\text{O})$ positions. Compared to the typical Lindqvist-type octahedral species $[\text{M}_6\text{O}_{19}]^{2-}$,⁴⁶⁻⁴⁸ two adjacent metallic atoms bear a Cp^* ligand in place of a terminal oxido ligand, leading to a neutral compound.

In addition to being isoelectronic with the Lindqvist-type $[\text{M}_6\text{O}_{19}]^{2-}$ ion, these neutral organometallic polyoxometallates are also isoelectronic with the known $[\text{Cp}^*\text{Mo}_6\text{O}_{18}]^-$ ion,^{49,50} which was best obtained as a Bu_4N^+ salt from $(\text{Bu}_4\text{N})[\text{MoCp}^*\text{O}_3]$ and $(\text{Bu}_4\text{N})_2[\text{Mo}_4\text{O}_{10}(\text{OMe})_4\text{Cl}_2]$ in methanol in up to 40% yield.⁵⁰ It seemed interesting to enlarge the synthetic spectrum of our aqueous $\text{Cp}^*_2\text{M}_2\text{O}_5/\text{M}'\text{O}_4^{2-}$ method to a stoichiometry of 1:10 for the rational synthesis of the $[(\text{Cp}^*\text{M})(\text{M}'\text{O})_5(\mu_2\text{-O})_{12}(\mu_6\text{-O})]^-$ (or $[\text{Cp}^*\text{MM}'_5\text{O}_{18}]^-$) ions, none of which has yet been described except for the above mentioned all-Mo example. We report in this paper the application of this strategy leading to the synthesis and

characterization of the entire series of $[\text{Cp}^*\text{MM}'_5\text{O}_{18}]^-$ ions ($\text{M}, \text{M}' = \text{Mo}, \text{W}$), obtained in the presence of a variety of different cations.

Results and Discussion

(a) Syntheses and characterization

The reaction between $\text{Cp}^*_2\text{M}_2\text{O}_5$ and $\text{M}'\text{O}_4^{2-}$ ($\text{M}, \text{M}' = \text{Mo}, \text{W}$) in a 1:10 molar ratio according to equation 1 selectively yields the anionic $[\text{Cp}^*\text{MM}'_5\text{O}_{18}]^-$ complexes in good yields and purity. The reaction is carried out by mixing the stoichiometric amounts of $\text{Cp}^*_2\text{M}_2\text{O}_5$ (dissolved in MeOH) and $\text{Na}_2\text{M}'\text{O}_4$ (aqueous solution), yielding the products after adequate acidification. The ions quantitatively precipitate upon addition of an appropriate organic halide salt. The cations used in this study are tetrabutylammonium **1a-4a**, tetrabutylphosphonium **1b-4b**, tetraphenylphosphonium **1c-4c**, or butyl-pyridinium in case of compounds **1d** and **3d**. The compounds colour varies from orange through pale green to yellow depending on the Mo/W ratio. Compound **1a** has already been previously reported and characterized, including by a single crystal X-ray diffraction study, but was synthesized by a different method in a lower yield (see Introduction).⁵⁰ The selectivity of the synthetic strategy is worthy of note: the reaction could have resulted, for instance, in a mixture of the previously reported $[\text{Cp}^*_2\text{M}_2\text{M}'_4\text{O}_{17}]$ compounds and the parent Lindqvist anions $[\text{M}'_6\text{O}_{19}]^{2-}$. This indicates the thermodynamic stability of the $[\text{Cp}^*\text{MM}'_5\text{O}_{18}]^-$ anions with respect to a hypothetical fragment redistribution process.



Compound	M	M'	Bu ₄ N	Bu ₄ P	Ph ₄ P	BuPyr
1	Mo	Mo	1a orange	1b orange	1c orange	1d orange
2	W	Mo	2a yellow	2b yellow	2c pale green	
3	Mo	W	3a pale green	3b pale green	3c pale green	3d pale green
4	W	W	4a pale yellow	4b pale yellow	4c pale yellow	

The success of this synthesis, as well as that of the related neutral $\text{Cp}^*_2\text{Mo}_x\text{W}_{6-x}\text{O}_{17}$ compounds,⁴⁵ relies on the high stability of Cp^*M bond in $\text{Cp}^*_2\text{M}_2\text{O}_5$ toward protonolysis at any pH.⁴³ Thus, it is possible to use the “ Cp^*M ” moieties as an elementary building block, especially at low pH, due to the ionic splitting of $\text{Cp}^*_2\text{M}_2\text{O}_5$ into $\text{Cp}^*\text{MO}_2(\text{H}_2\text{O})^+$ and Cp^*MO_2^+ . The occurrence of this process was clearly demonstrated for the Mo system^{43,51} and ^1H NMR evidence shows that it also takes place for the W system.⁵² Thus, the syntheses performed herein can be considered as the assembly of individual organometallic $\{\text{Cp}^*\text{MO}_2\}^+$ fragments and inorganic $\{\text{M}'\text{O}_4\}^{2-}$ species, using specific stoichiometry and pH conditions. The products are stable in water at low pH. Three of the compounds were obtained in the form of single crystals; their molecular structures will be described in the next section.

The ^1H NMR spectra of the isolated salts in DMSO show the Cp^* signal at δ 2.2 (when linked to Mo) or 2.4 (when linked to W), plus the resonances of the cation with suitable intensity for the 1:1 $\text{Cp}^*/\text{cation}$ stoichiometry. The ^{31}P NMR spectrum of the phosphonium salts shows the expected cation resonance at δ 23.4 for Ph_4P^+ and 35.1 for Bu_4P^+ . The compounds show characteristic $\text{M}=\text{O}$ and $\text{M}-\text{O}-\text{M}$ vibrations in the IR spectrum. These will be analyzed in detail later in section *d* on the basis of the DFT calculations. All compounds were also investigated in terms of their thermal behaviour by thermogravimetric analyses (TGA) in air. The salts with N-based cations (**a**, **d**) led to complete loss of the organic part, with formation of the mixed-metal trioxides $\text{M}_{x/6}\text{M}'_{1-x/6}\text{O}_3$ ($x = 0, 1, 5, 6$), with a relative good match between experimentally observed and theoretical mass losses upon warming up to 500°C . The TGA analysis of the salts with phosphonium cations (**b**, **c**) gave indication of phosphorus loss or not depending on the anion (P_2O_3 is volatile at the temperatures used in the experiments) but a precise stoichiometry could not be established.

All anions were also investigated by mass spectrometry using electrospray method. The spectrum in negative mode showed the expected molecular ion with an isotopic pattern in

good agreement with the simulation, see Figure 1. Notably, metal compositions different from MM'_5 (for instance $M_2M'_4$) were absent from the spectra of the mixed-metal products **2** and **3**. The fragmentation pattern is not identical for each type of anion, but as a general feature we can observe loss of the Cp^* fragment to yield $[MM'_5O_{18}]^-$, followed by subsequent loss of both MO_3 and $M'O_3$.

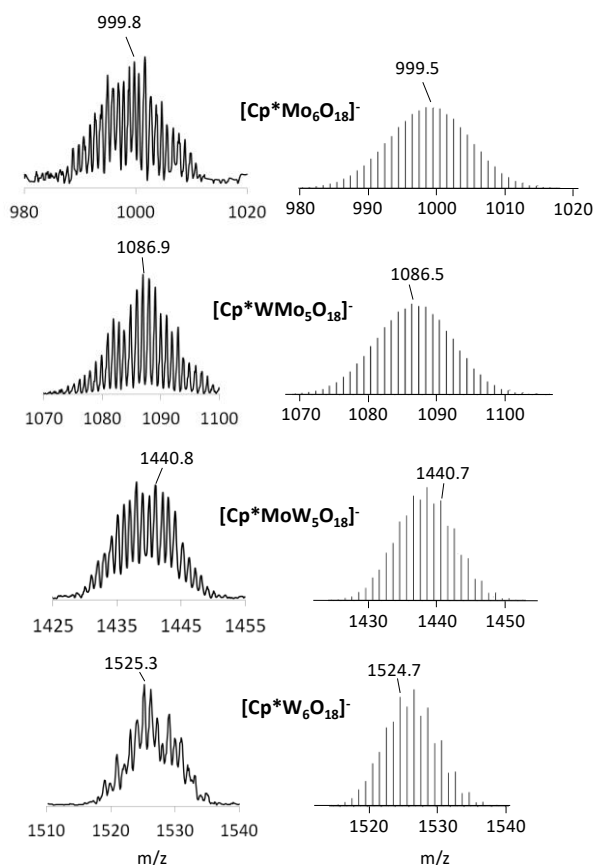
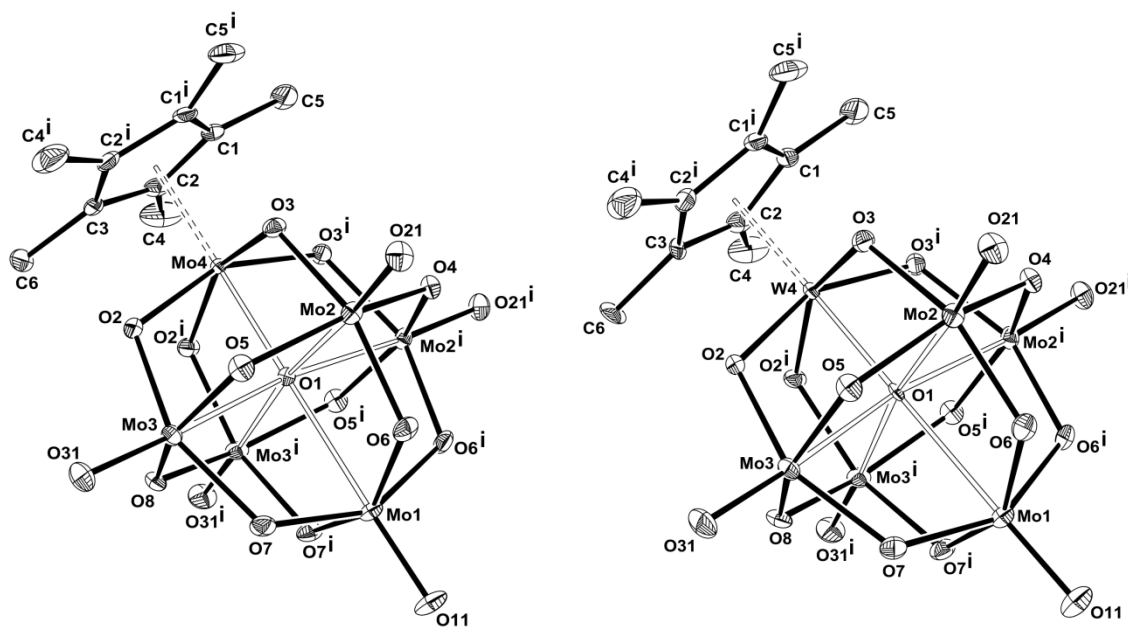


Figure 1. Experimental (left) and simulated (right) isotopic patterns for the $[Cp^*Mo_xW_{6-x}O_{18}]^-$ ions measured for compounds **1a**, **2b**, **3b** and **4c** by electrospray mass spectrometry (negative mode) in acetone/methanol solution.

(b) X-ray diffraction studies

The PPh_4^+ salts of the $[Cp^*Mo_6O_{18}]^-$ (**1c**) and $[Cp^*WMo_5O_{18}]^-$ (**2c**) anions as well as the nBu_4N^+ salt of $[Cp^*WMo_5O_{18}]^-$ (**2a**) gave single crystals suitable to X-ray diffraction analyses. The two tetraphenylphosphonium salts **1c** and **2c** are isomorphous and crystallise

with one molecule of interstitial acetone. Compound **2a**, on the other hand, is not isostructural with the previously characterized $[\text{Cp}^*\text{Mo}_6\text{O}_{18}]^-$ salt **1a**. The polyanions have the typical Lindqvist-type octahedral arrangement of the 6 metal atoms and bridging oxygen atoms, with one $\{\text{Mo}=\text{O}\}^{4+}$ fragment in $[\text{Mo}_6\text{O}_{19}]^{2-}$ being formally replaced by a $\{\text{Cp}^*\text{Mo}\}^{5+}$ (in **1c**) or $\{\text{Cp}^*\text{W}\}^{5+}$ (in **2a** and **2c**) fragment. Views of the geometry of both anions are available in Figure 2. For compounds **1c** and **2c**, the asymmetric unit contains half of the anionic cluster (and half of the cation), with atoms Mo1, M4 (M = Mo or W), O1, O4, O8, O11, C3 and C6 sitting on a crystallographic mirror plane. The structure of **2a**, on the other hand, contains the entire molecule in the asymmetric unit, which therefore does not display any crystallographically imposed symmetry.



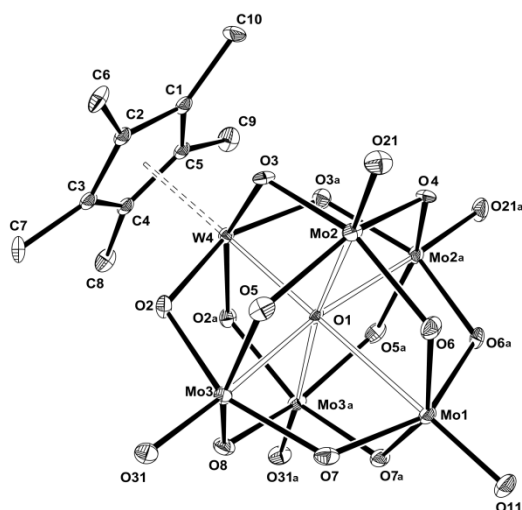


Figure 2. ORTEP views of the $[\text{Cp}^*\text{MMo}_5\text{O}_{18}]^-$ ions. (a) $M = \text{Mo}$ in compound **1c**; (b) $M = \text{W}$ in compound **2c**; (c) $M = \text{W}$ in compound **2a**. The ellipsoids are drawn at the 30% probability level and the Cp^* H atoms are not shown.

Table 1 reports the relevant bond distances (angles are in the SI, Table S1). The numbering scheme used for the anions in compounds **1c** and **2c** is identical (with the metal atom M4 being Mo in **1c** and W in **2c**). The numbering scheme of the anion in **2a** is the same as the other two anions for what concerns the first half of the molecule and only this half is described in Table 1 in comparison with the other two structures. The opposite half has metric parameters in close correspondence with the first one, in spite of the absence of crystallographic mirror symmetry in this case. A full table of bond distances and angles of **2a** is available in the Supporting Information (Table S1) and all distances are also displayed later in the DFT section. The $\text{Cp}^*\text{-M}$ distance is slightly shorter when $M = \text{W}$. All structurally equivalent M-O bonds have quite similar distances in the two compounds. The ideal C_{4v} symmetry of the ions, however, is broken by a distortion that renders the bridging Mo-O-Mo moieties asymmetric and this distortion is more pronounced in compound **1** than in compound **2**. This distortion will be further discussed later in the DFT section. In addition, the central ($\mu_6\text{-O}$) atom is drawn closer to the $\text{Cp}^*\text{-bearing}$ axial metal (Mo(4) in **1c** and W(4) in **2c**) and farther away from the opposite axial Mo(1) atom, the distances to the equatorial Mo(2) and

Mo(3) atoms being intermediate. This type of distortion is however less pronounced than in the Cp*₂Mo₆O₁₇ structure.⁴⁴

Table 1. Relevant bond lengths [Å] for all structures.^a

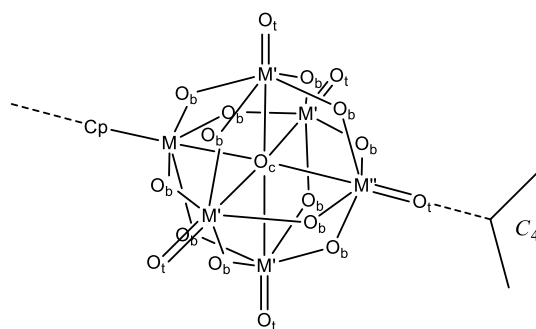
	1c (M(4) = Mo)	2c (M(4) = W)	2a (M(4) = W)
Distances			
Mo(1)-O(1)	2.504(3)	2.512(4)	2.502(7)
Mo(1)-O(6)	1.923(2)	1.914(4)	1.894(8)
Mo(1)-O(7)	1.878(2)	1.899(4)	1.911(8)
Mo(1)-O(11)	1.673(3)	1.669(5)	1.688(8)
Mo(2)-O(1)	2.3285(19)	2.335(3)	2.343(7)
Mo(2)-O(3)	1.908(2)	1.898(3)	1.911(8)
Mo(2)-O(4)	1.9287(15)	1.933(3)	1.939(7)
Mo(2)-O(5)	1.928(2)	1.931(4)	1.950(8)
Mo(2)-O(6)	1.890(2)	1.894(3)	1.918(8)
Mo(2)-O(21)	1.679(2)	1.678(4)	1.667(7)
Mo(3)-O(1)	2.3391(19)	2.346(3)	2.338(6)
Mo(3)-O(2)	1.870(2)	1.883(3)	1.912(8)
Mo(3)-O(5)	1.933(2)	1.941(4)	1.947(8)
Mo(3)-O(7)	1.928(2)	1.908(3)	1.898(9)
Mo(3)-O(8)	1.9317(15)	1.937(3)	1.957(7)
Mo(3)-O(31)	1.674(2)	1.671(4)	1.683(7)
M(4)-O(1)	2.109(3)	2.104(4)	2.136(7)
M(4)-O(2)	1.974(2)	1.958(3)	1.925(7)
M(4)-O(3)	1.917(2)	1.931(3)	1.934(8)
M(4)-Ct(1)	2.092(2)	2.085(2)	2.105(4)

^a The bond angles are provided in the Supporting Information (Table S1). Ct = Cp* ring centroid.

(c) DFT calculations

By analogy with the previously reported mixed-metal neutral compounds,⁴⁵ DFT geometry optimizations were carried out on the isoelectronic anionic [Cp*MM'₅O₁₈]⁻ complexes in order to interpret the IR absorption spectrum in the M=O stretching region and to understand the effect on them of the metal nature. To save computational time, simplified

models were used where the Cp* ligands were replaced by Cp rings. The models are numbered by roman numerals corresponding to the compounds numbering scheme: $[\text{CpMo}_x\text{W}_{6-x}\text{O}_{18}]^-$ with $x = 6$ (**I**), 5 (**II**), 1 (**III**) and 0 (**IV**). If we consider free rotation of the Cp ligand linked to M, the cluster geometry can be idealized to C_{4v} . This is justified at least on the NMR timescale, because the five methyl groups of the Cp* ligands are equivalent in the ^1H NMR spectrum. In order to facilitate the discussion, the five (M=O) metals will be labelled according to their idealized symmetry equivalence: M' is used for the four equivalent equatorial metals and M'' for the axial metal *trans* to the M atom that bears the Cp ring. The terminal O atoms will be labelled O_t , the doubly bridging atoms O_b and the central ($\mu_6\text{-O}$) atom O_c (see Scheme 1). No symmetry constraint was imposed to the ions during the geometry optimizations. The full Cartesian coordinates of the optimized geometries are available in the Supporting Information (Table S2) and relevant metric parameters are summarized in Table 2. For comparison, Table 2 reports also all distances of the three structures described in this contribution, as well as the previously described structure of **1a**.⁵⁰



Scheme 1. Atom labelling scheme used in Table 2.

Table 2. Selected bond distances for the geometry optimized models **I-IV** and comparison with the experimental structures of **1c** and **2c**.^[a]

System	1a ^[b]	1c	I	2a	2c	II	III	IV
M		Mo	Mo	W	W	W	Mo	W
M'=M''		Mo	Mo	Mo	Mo	Mo	W	W

M-Cp	2.08(3)	2.092(2)	2.150	2.105(4)	2.085(2)	2.163	2.139	2.151
	1.65(2)	1.674(2)	1.688	1.667(7)	1.678(4)	1.687	1.701	1.701
M'-O _t	1.67(2)		1.688	1.675(7)		1.687	1.701	1.701
	1.68(2)	1.679(2)	1.688	1.676(7)	1.671(4)	1.687	1.701	1.701
	1.68(2)		1.688	1.683(7)		1.687	1.701	1.701
M''=O _t	1.62(2)	1.673(3)	1.681	1.688(8)	1.669(5)	1.681	1.696	1.696
M-O _c	2.14(1)	2.109(3)	2.074	2.136(7)	2.104(4)	2.067	2.127	2.103
	2.33(1)	2.328(2)	2.378	2.338(6)	2.335(3)	2.369	2.365	2.369
M'-O _c	2.33(1)		2.382	2.338(6)		2.372	2.366	2.370
	2.33(1)	2.339(2)	2.383	2.343(7)	2.346(3)	2.379	2.367	2.370
	2.34(2)		2.386	2.353(6)		2.380	2.368	2.375
M''-O _c	2.48(1)	2.504(3)	2.609	2.502(7)	2.512(4)	2.629	2.585	2.602
	1.87(2)	1.917 (2)	1.886	1.921(7)	1.931(3)	1.910	1.915	1.918
M-O _{b(M')}	1.88(2)		1.890	1.925(8)		1.921	1.923	1.927
	1.91(2)	1.974 (2)	1.995	1.934(7)	1.958(3)	1.946	1.947	1.940
	1.94(2)		2.009	1.952(8)		1.964	1.962	1.951
	1.90(2)	1.870 (2)	1.881	1.906(8)	1.883(3)	1.910	1.914	1.921
M'-O _{b(M)}	1.92(2)		1.881	1.911(8)		1.927	1.926	1.930
	1.93(2)	1.908 (2)	1.990	1.912(8)	1.898(3)	1.951	1.947	1.942
	1.95(2)		1.990	1.918(8)		1.962	1.954	1.950
	1.90(2)	1.928(2)	1.837	1.933(8)	1.931(3)	1.924	1.924	1.926
	1.92(2)		1.838	1.936(7)		1.924	1.925	1.926
M'-O _{b(M')}	1.93(2)	1.929(2)	1.843	1.939(7)	1.933(4)	1.924	1.926	1.927
	1.94(2)		1.845	1.947(8)		1.925	1.929	1.927
	1.94(2)	1.932(2)	2.043	1.949(7)	1.937(4)	1.935	1.929	1.930
	1.95(2)		2.044	1.950(8)		1.935	1.931	1.931
	1.96(2)	1.933(2)	2.051	1.957(8)	1.941(3)	1.936	1.932	1.932
	1.96(2)		2.059	1.957(7)		1.937	1.934	1.933
	1.94(2)	1.890(2)	1.875	1.898(9)	1.894(3)	1.902	1.906	1.910
M'-O _{b(M'')}	1.95(2)		1.883	1.913(8)		1.912	1.913	1.916
	1.97(2)	1.928(2)	1.968	1.918(8)	1.908(3)	1.934	1.930	1.928
	1.97(2)		1.976	1.919(8)		1.950	1.941	1.935
	1.84(2)	1.878(2)	1.875	1.894(8)	1.899(4)	1.895	1.903	1.907
	1.85(2)		1.880	1.902(8)		1.909	1.913	1.913
M''-O _{b(M')}	1.86(2)	1.923(2)	1.963	1.911(8)	1.914(4)	1.932	1.929	1.926
	1.87(2)		1.975	1.915(8)		1.943	1.937	1.932

[a] For the definition of the symbols used, see Scheme 1. [b] From ref. ⁵⁰.

The agreement between experimental and calculated geometries for the [MM'₄M''O₁₈]⁻ core in the case of **1**/**I** and **2**/**II** is generally quite good. The calculated distances to the terminal and bridging ligands are generally only slightly longer than the experimentally

observed ones (the maximum deviation is 0.05 Å for M-O_{b(M')} and M''-O_{b(M)} in **I**), whereas the distances to the central O atom are slightly underestimated for M-O_c (by 0.01 Å). As for neutral compounds, the atom O_c is much closer to M than to M' and M'' and the calculations tend to place O_c even closer to M relative to the experimental structure. This discrepancy could of course be related to the use of the simplified model.

The experimentally observed asymmetry of the central MM'₄M''O₁₈ core is also shown in the optimized structure and decreases, in agreement with the experimental observations, upon replacing Mo with W atoms in the structure, tending toward the symmetric limiting structure for the all-W member of the series. A trans-alternation pattern of long and short bond lengths in {M₄(O_b)₄} rings yielding distorted octaedra, originally described for the parent Lindqvist anions,⁵³ is a common feature of polyoxometalates and is notoriously more pronounced for molybdates than for tungstates. However, formal replacement of a terminal oxo ligand by a Cp ring,⁵⁴ as in [CpTiM₅O₁₈]³⁻, or an imido group,^{55,56} as in [M₆O₁₈(NAr)]²⁻ (M = Mo, W) appears to somewhat attenuate this irregularity. The introduction of a single W atom renders the structures of **2a** and **2c** very close to the symmetric limit and the optimized anion structure (**II**) is also very little distorted. The reason for this trend is not quite clear and its understanding goes beyond the scope of the present work. This trend has also been noted for the isoelectronic Cp*₂Mo_xW_{6-x}O₁₇ series.⁴⁵ However, a close analysis of this asymmetry for compounds **1/I** reveals interesting features. The asymmetry is most clearly visible in the distances between the O_b atoms and the metal atoms. The two experimental structures and the optimized geometry, however, exhibit three different kinds of asymmetry. Focusing first on the M'-O_b-M'' moieties, the structure of **1a**, although of low quality, shows that the four independent M'-O_{b(M')} distances have a narrow spread around their average, 1.96(2) Å, and the same is true for the M''-O_{b(M'')} distances, 1.86(2), while these two averages are very different from each other. For the structure of **1c**, on the other hand, the asymmetry is

manifested within each set of structurally equivalent distances. The optimized distances in **I** follow the same trend as **1c**. For the M'-O_b-M' moieties, however, the situation is quite different. There is an insignificant distortion in both experimental structures (averages of 1.94(2) Å for **1a** and 1.930(2) Å for **1c**), whereas the calculated distances in **I** yield two very different sets of four distances each, with averages 1.841(4) and 2.049(7) Å. Finally, the M-O_b-M' moieties show the same type of distortion in all three geometries, namely two sets of two different distances for each structurally equivalent M-O_{b(M')} and M'-O_{b(M)} set, the difference between the short and long sets being smaller for **1a** (0.04(2) and 0.03(2) Å), intermediate for **1c** (0.057(2) and 0.038(2) Å), and greater for **I** (0.11(1) and 0.110 Å). This analysis clearly shows that there is a driving force for the POM structure to distort away from maximum symmetry, not solely related to crystal packing. However, the crystal packing (nature of the cation) has the effect of driving this distortion in different directions. The effect of packing forces is also revealed by the discrepancy in the experimental structures (Table 1) between the W4-Ct distances in compounds **2a** and **2c**.

We also wish to note that the effect of the metal nature on the distortion of the octahedral M₆(O_b)₁₂ scaffold is also quite evident for the parent [M₆O₁₉]²⁻ Linqvist anions (M = Mo, W). The statistical analysis of all the salts of these two dianions for which a structure is reported in the Cambridge Structural Database shows a greater average distortion for the Mo structure relative to the W structures. Of the 77 Mo structure, the difference between the maximum and minimum Mo-O_b distances (Δ) goes from zero (for the hydrated NEt₄⁺ salt where the dianion sits on a crystallographic $m\bar{3}m$ position)⁵⁷ to a maximum of 0.22 Å (for a crown ether-containing ammonium salt)⁵⁸ with an average Δ of 0.104 Å over the entire set. In the most distorted structure, two equal sets of short, 1.85(2) Å, and long, 2.01(3) Å, Mo-O_b distances can be identified like for the [Cp*Mo₆O₁₈]⁻ structures analyzed here. For the 70 W structures, on the other hand, the average Δ is reduced to 0.060 Å. Like for the

[Cp*MM'₄M''O₁₈]⁻ ions analyzed in this contribution, the nature of the cation and the consequent packing forces seem to greatly influence the degree of distortion, since both undistorted Mo structure (see above) and very distorted W structures (such as the Et₄N⁺ salt with $\Delta = 0.21 \text{ \AA}$)⁵⁹ exist. It can be concluded that this structural motif has a natural tendency to distort from the maximum symmetry but the potential energy surface along this distortion is rather flat, allowing a great degree of control to be exerted by the crystal packing. The greater average distortion for the Mo structures is probably caused by the weakness of the Mo-O_b bonds relative to the W-O_b bonds.

The trends of the bond distances, beyond the above discussed asymmetry, due to the change of M or M'/M'' along the series of structures **I-IV** can be divided into primary (distances to the metal being changed) and secondary (distances to M due to a change of M'/M'', or viceversa) effects. The calculations show similar trends to those already observed for the neutral [Cp₂M₂M'₂M''₂O₁₇] analogues.⁴⁵ The primary effect is relative important in the M-Cp distance ($\Delta = 0.013$ from **I** to **II** and 0.012 from **III** to **IV**), but a secondary effect in the same distance is also notable ($\Delta = -0.011$ from **I** to **III** and -0.012 from **II** to **IV**). In other words, the M-Cp distance is lengthened on going from Mo to W, but is shortened when the M'/M'' atoms are changed from Mo to W. On going from Mo to W, the terminal M'/M''=O_t distances show a slight primary lengthening and no significant secondary effects. Conversely, the M-O_c and M''-O_c show a primary shortening and a slight secondary lengthening, whereas no large effects are visible in the M'-O_c distances.

(d) IR characterization

Infrared spectroscopy is a good characterization tool for symmetrical polyanions. For the Lindqvist M₆O₁₉²⁻ anions (M = Mo, W), the number of observed vibrations is determined by their *O_h* symmetry^{60,61} and a correlation between experimental and calculated vibrations

could be established.⁶² As already discussed above, the symmetry of the polyoxometallate cluster in compounds **1-4** is reduced at best to C_{4v} (considering Cp* as a rapidly rotating ligand). The observed structures, backed up by the DFT calculations, show however a further symmetry reduction to C_s , which is more pronounced for the Mo-richer compounds.

The observed (for **1a-4a**) and calculated (for **I-IV**) IR spectra in the metal-oxygen stretching region are shown in Figure 3 (see Experimental section for the list of frequencies) and the calculated frequencies, symmetry labels and assignment are listed in Table 3. Views of the normal modes are shown in the Supporting Information (Table S3). As found for all POM derivatives, the terminal $M^{\prime}=O_t$ and $M^{\prime\prime}=O_t$ vibrations have higher frequency (observed, 950-1000 cm^{-1} ; calculated, 1020-1050 cm^{-1}) than the $M-O_b-M$ vibrations (observed 750-890 cm^{-1} , calculated 780-850 cm^{-1}). Some contribution of Cp C-H bending modes is found to mix with the lowest frequency vibration (840-960 cm^{-1}). There is a rather good match between calculated and observed spectra (Figure 3), the frequency shift certainly being related the computational method and/or to the model (Cp vs. Cp*). This gives us confidence in the reported band assignment.

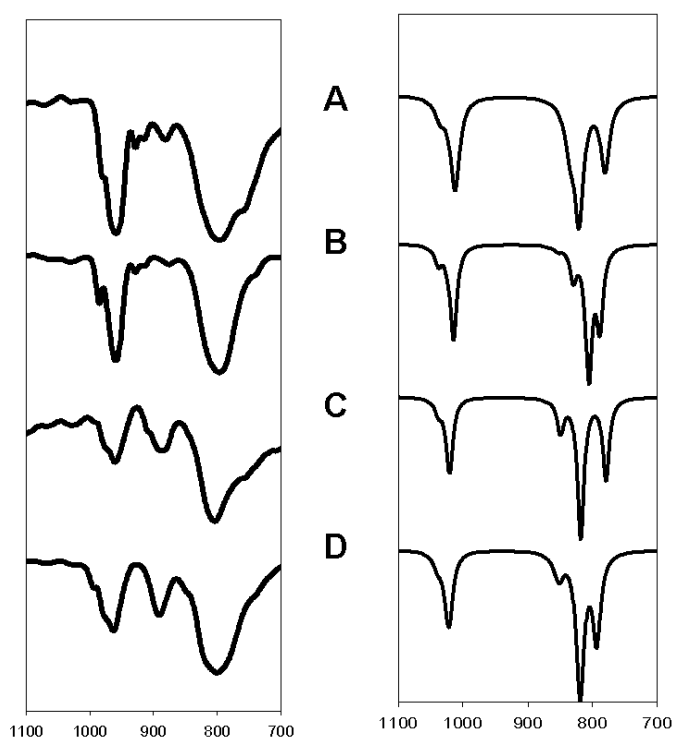


Figure 3. Experimental (left) and DFT calculated (right) IR spectra in the Mo-O stretching region for compounds **1a/I** (A), **2a/II** (B), **3a/III** (C), **4a/IV** (D). The range 700-1100 cm^{-1} correspond to the higher frequencies observed for M=O and M-O-M vibrations.

Table 3. Calculated vibrations (cm^{-1}) in the M-O stretching region with relative intensities (KM/Mole) in parentheses.

I	II	III	IV	Symmetry ^[a]	Assignment
780 (842)	788 (903)	779 (949)	793 (1023)	A ₁	(M-O-M') _s + Cp
820 (703)	805 (769)	818 (824)	819 (843)	E	(M _t -O-M _t) ^[b]
821 (715)	806 (756)	818 (824)	819 (842)		
835 (94)	813 (17)	836 (1)	838 (1)	B ₁	(M _t -O-M _t) _{as} ^[b]
835 (343)	829 (360)	849 (331)	851 (251)	A ₁	(M'-O-M'') _s
1011 (34)	1013 (26)	1019 (1)	1020 (5)	B ₁	(M'=O) _{as}
1012 (528)	1014 (536)	1020 (426)	1021 (426)	E	(M'=O)
1012 (498)	1015 (535)	1020 (425)	1022 (422)		
1021 (68)	1024 (82)	1027 (62)	1028 (64)	A ₁	(M'=O) _s - (M''=O)
1035 (215)	1038 (199)	1038 (156)	1031 (149)	A ₁	(M'=O) _s + (M''=O)

The trends of calculated frequencies as the metal atoms are changed are amenable to a detailed analysis. First of all, the structural distortion away from the idealized C_{4v} symmetry, even for system **I** where this distortion is more pronounced (see previous section), is not significantly reflected in the shape of the normal modes. For instance, the pseudo-degenerate E-type modes, which split into $A'+A''$ in C_s symmetry, remain practically degenerate (maximum difference: 1 cm^{-1}). Therefore, the labels of the higher symmetry C_{4v} point group are used in Table 3 and in the discussion. Five terminal metal-oxido ($M'=O$ and $M''=O$) vibrations are expected and indeed found by the calculations ($2A_1+B_1+E$). The B_1 band, corresponding to $\nu_{as}(M'=O)$, is very weak due to small overall dipole moment, whereas the E-type pair has the highest intensity. The two A_1 -type vibrations correspond to the in-phase (stronger) and out-of-phase (weaker) elongations of the $M'=O$ and $M''=O$ bonds. Thus, only three major bands are essentially observed in this region. The calculated frequencies do not show significant trend as a function of the metal nature. The analysis of the bridging Mt-O-Mt vibrations ($Mt = M, M'$ or M'') is more complex, because of more extensive vibrational coupling not only among structurally different bonds but also with vibration of other nature (notably Cp bending modes). The five most representative bands ($2A_1+B_1+E$) are listed in Table 3.

From the experimental spectra only two $\nu(M=O)$ bands can be unambiguously determined, sometimes with shouldering. Comparison with the calculated spectra suggest that the strongest one is the E-type vibration, whereas the second most intense band is most probably the highest frequency A_1 -type band. Experimentally, the most significant effect on the spectrum in this region is seen for a change of the inorganic metal, whereas a change of the organometallic one produces hardly any difference.

Conclusions

We have presented here a new, rational and facile synthesis of new organometallic Group 6 Lindqvist-type polyanions of type $[\text{Cp}^*\text{MM}'_5\text{O}_{18}]^-$ ($M, M = \text{Mo}, \text{W}$). This family was previously represented only by the homometallic Mo member, obtained by two different and less efficient synthetic strategies. The thermal decomposition of these compounds (at least those with N-containing cations) yields the mixed-metal oxides $\text{M}_{x/6}\text{M}'_{1-x/6}\text{O}_3$ with a homogeneous distribution of the two metals, which may be of interest for the study of the metal influence in various applications.

Experimental Section

All experiments were performed in air. Compounds $\text{Cp}^*_2\text{Mo}_2\text{O}_5$ and $\text{Cp}^*_2\text{W}_2\text{O}_5$ were synthesized according to the literature.⁶³ Water was deionized and methanol (Carlo Erba, analytical grade) was used as received. Sodium molybdate and tungstate dihydrates ($\text{Na}_2\text{MO}_4 \cdot 2\text{H}_2\text{O}$, $M = \text{Mo}, \text{W}$), tetrabutylammonium bromide (Bu_4NBr), tetrabutylphosphonium bromide (Bu_4PBr), tetraphenylphosphonium bromide (Ph_4PBr) and N-butylpyridinium bromide (BuPyrBr) were purchased from Aldrich and used as received. Elemental analyses (C, H and N) were performed by the LCC Analytical Service Laboratory. The IR spectra were recorded on KBr pellets at room temperature with a Mattson Genesis II FTIR spectrometer and the data were processed with WinFirst software. The TGA measurements were carried out on a SDT Q600 V20.9 thermal analyzer. A quantity of each sample was placed into a nickel/platinum alloy crucible and heated at $0.83 \text{ K} \cdot \text{s}^{-1}$ under reconstituted air flow up to 500 K. An empty crucible was used as a reference. ^1H and ^{31}P NMR spectra were on a Bruker Avance DPX-200 spectrometer. Mass spectrometry analyses were performed at

the “Service Commun de Spectrométrie de Masse » of Université Paul Sabatier on a API 365 Perkin Elmer Mass spectrometer, in electrospray ionization mode and negative polarity.

General synthetic procedure of Cat[Cp*MM’₅O₁₈]. The same procedure was used for all compounds. One equivalent of Cp*M₂O₅ (M = Mo or W) was dissolved in the minimum amount of methanol. In a second flask, ten equivalents of Na₂M’O₄·2H₂O (M’ = Mo or W) were dissolved in the minimum amount of water. Both solutions were mixed without apparent change. Aqueous 1 M HNO₃ (18 equivalents) was then added to the mixture, resulting in a color change (the color depends on the M/M’ nature, see equation 1). The mixture was left stirring at room temperature for two hours. The bromide salt with the desired (> 3 equivalents) dissolved in water was then added to the solution leading to a precipitate of the expected compound. The product was filtered off, washed with small portions of water, methanol and diethylether and finally dried under vacuum at 70°C.

Bu₄N[Cp*Mo₆O₁₈], 1a. 92% yield. IR (ν, cm⁻¹): 979sh, 957s, 796s. Anal. Calc. for C₂₆H₅₁O₁₈NMo₆: C, 25.1; H, 4.1; Found: C, 25.1; H, 4.1 TGA: formal loss Bu₄NCp*; % exp. (calcd): 30.5 (30.4). ¹H NMR (DMSO-*d*₆): δ 0.96 (q, 12H, Me), 1.35 (m, 8H, CH₂), 1.59 (m, 8H, CH₂), 2.27 (s, 15H, Cp*), 3.18 (m, 8H, CH₂). MS: m/z = 999.8 (theor. 999.5), [Cp*Mo₆O₁₈]⁻.

Bu₄P[Cp*Mo₆O₁₈], 1b. 92% yield. IR (ν, cm⁻¹): 979sh, 967s, 916sh, 798s, 759sh. Anal. Calc. for C₂₆H₅₁O₁₈PMo₆: C, 24.8; H, 4.1. Found: C, 25.0; H, 3.8. TGA: loss of 4 Bu and Cp*; % exp. (calcd): 28.3 (28.9). ¹H NMR (DMSO-*d*₆): δ 0.94 (q, 12H, Me), 1.46 (m, 8H, CH₂), 2.20-2.30 (m, 16H, CH₂), 2.27 (s, 15H, Cp*). ³¹P NMR (DMSO-*d*₆): δ 35.1.

Ph₄P[Cp*Mo₆O₁₈], 1c. 92% yield. IR (ν, cm⁻¹): 967s, 878s, 796s, 760sh. Anal. Calc. for C₃₄H₃₅O₁₈PMo₆: C, 30.5, H 2.6. Found: C, 30.2; H, 2.8. TGA: formal loss of Ph₄PCp*; % exp. (calcd): 35.3 (35.4). ¹H NMR (DMSO-*d*₆): δ 2.27 (s, 15H, Cp*), 7.6-8.2 (m, 15H, Ar). ³¹P NMR (DMSO-*d*₆): δ 23.6. Single crystals of this compound could be grown from acetone.

BuNC₅H₅[Cp*Mo₆O₁₈], 1d. 93% yield. IR (ν , cm⁻¹): 962l, 782s, 757sh. Anal. Calc. for C₁₉H₂₉O₁₈NMo₆: C, 20.1; H, 2.6. Found: C, 20.9; H, 2.5. TGA: formal loss of (BuNC₅H₅)Cp*; % exp. (calcd): 24.5 (23.9). ¹H NMR (200 MHz, DMSO-*d*₆): δ 0.93 (q, 3H, Me), 1.31 (m, 2H, CH₂), 2.20 (m, 2H, CH₂), 2.27 (s, 15H, Cp*), 4.61 (m, 2H, CH₂), 8.18 (m, 2H, CH_{pyr}), 8.63 (m, 1H, CH_{pyr}), 9.10 (m, 2H, CH_{pyr}).

Bu₄N[Cp*Mo₅WO₁₈], 2a. 79% yield. IR (ν , cm⁻¹): 984sh, 954s, 797s. Anal. Calc. for C₂₈H₅₇O₁₉NMo₅WO₁₈: C, 23.5; H, 3.9. Found: C, 24.1; H, 3.7. TGA: formal loss of Bu₄NCp*; exp. (calcd): 28.6 (28.4). ¹H NMR (DMSO-*d*₆): δ 0.95 (q, 12H, Me), 1.34 (m, 8H, CH₂), 1.59 (m, 8H, CH₂), 2.41 (s, 15H, Cp*), 3.19 (m, 8H, CH₂). Single crystals of this compound could be grown from acetone.

Bu₄P[Cp*Mo₅WO₁₈], 2b. 55% yield. IR (ν , cm⁻¹): 984sh, 961s, 796s, 721sh. Anal. Calc. for C₂₆H₅₁O₁₈PMo₅W: C, 23.2; H, 3.8. Found: C, 23.6; H, 3.6. TGA: formal loss of Cp*, and 4 Bu; % exp. (calcd): 28.1 (27.0). ¹H NMR (DMSO-*d*₆): δ 0.95 (q, 12H, Me), 1.47 (m, 8H, CH₂), 2.17 (m, 2H, CH₂), 2.17 (s, 15H, Cp*). ³¹P NMR (DMSO-*d*₆): δ 35.2. MS: *m/z* = 1086.9 (theor. 1086.5), [Cp*WMo₅O₁₈]⁻.

Ph₄P[Cp*Mo₅WO₁₈], 2c. 48 % yield. IR (ν , cm⁻¹): 983sh, 958s, 883s, 795s. Anal. Calc. for C₃₄H₃₅O₁₈PMo₅W: C, 28.6; H, 2.5. Found: C, 25.9; H, 2.2. TGA: formal loss of Ph₄PCp*; % exp. (calcd): 31.9 (33.2). ¹H NMR (DMSO-*d*₆): δ 2.3 (s, 15H, Cp*), 7.6-8.1 (m, 15H, Ar). ³¹P NMR (DMSO-*d*₆): δ 23.4.

Bu₄N[Cp*MoW₅O₁₈], 3a. 78% yield. IR (ν , cm⁻¹): 995sh, 961s, 886s, 805s. The compound was recrystallized from acetone and its elemental analysis was carried out on crystals of [Bu₄N][Cp*MoW₅O₁₈] \cdot acetone (C₂₉H₅₇O₁₉NMoW₅). Anal. Calcd.: C, 20.0; H, 3.3. Found: C, 20.7; H, 3.6. TGA: formal loss of Bu₄NCp*; % exp. (calcd): 23.7 (22.5). ¹H NMR (DMSO-*d*₆): δ 0.96 (q, 12H, Me), 1.35 (m, 8H, CH₂), 1.59 (m, 8H, CH₂), 2.17 (s, 15H, Cp*), 3.19 (m, 8H, CH₂).

Bu₄P[Cp*MoW₅O₁₈], 3b. 80% yield. IR (ν , cm^{-1}): 956s, 796s. Anal. Calcd. for $\text{C}_{26}\text{H}_{51}\text{O}_{18}\text{PMoW}_5$: C, 18.4; H, 3.0. Found: C, 19.0; H, 3.3. TGA: formal loss of Cp* and 4 Bu; % exp. (calcd): 23.4 (21.4). ^1H NMR ($\text{DMSO-}d_6$): δ 0.96 (q, 12H, Me), 1.46 (m, 8H, CH₂), 1.59 (m, 8H, CH₂), 2.17-2.21 (m, 23H, CH₂ + Cp*), ^{31}P NMR ($\text{DMSO-}d_6$): δ 35.1. . MS: $m/z = 1440.8$ (theor. 1440.7), $[\text{Cp}^*\text{MoW}_5\text{O}_{18}]^-$.

Ph₄P[Cp*MoW₅O₁₈], 3c. 95% yield. IR (ν , cm^{-1}): 960sh, 794s. Anal. Calcd. for $\text{C}_{34}\text{H}_{35}\text{O}_{18}\text{PMoW}_5$: C, 23.0; H, 2.0. Found: C, 24.1; H, 1.8. TGA: formal loss of Ph₄PCp*; % exp. (calcd): 27.9 (26.6). ^1H NMR ($\text{DMSO-}d_6$): δ 2.4(s, 15H, Cp*), 7.6-8.1 (m, 15H, Ar), ^{31}P NMR ($\text{DMSO-}d_6$): δ 23.6..

BuNC₅H₅[Cp*MoW₅O₁₈], 3d. 93% yield. IR (ν , cm^{-1}): 958sh, 804s. Anal. Calc. for $\text{C}_{19}\text{H}_{29}\text{O}_{18}\text{NMoW}_5$: C, 14.5; H, 1.9. Found: C, 15.0; H, 2.2. TGA: formal loss of BuNC₅H₅Cp*; % exp. (calcd): 19.5 (17.2). ^1H NMR ($\text{DMSO-}d_6$): δ 0.95(q, 3H, Me), 1.32 (m, 2H, CH₂), 2.20 (m, 2H, CH₂), 2.27 (s, 15H, Cp*), 4.61 (m, 2H, CH₂), 8.21 (m, 2H, CH_{pyr}), 8.64 (m, 1H, CH_{pyr}), 9.12 (m, 2H, CH_{pyr}).

Bu₄N[Cp*W₆O₁₈], 4a. 83% yield. IR (ν , cm^{-1}) 991s, 960s, 892s 798s. Anal. Calc. for $\text{C}_{26}\text{H}_{51}\text{O}_{18}\text{PW}_6$: C, 17.6; H, 2.9. Found: C, 18.7; H, 2.9. TGA: formal loss of Bu₄NCp* % exp. (calcd): 21.4 (21.3). ^1H NMR ($\text{DMSO-}d_6$): δ 0.96 (q, 12H, Me), 1.35 (m, 8H, CH₂), 1.59 (m, 8H, CH₂), 2.17 (s, 15H, Cp*), 2.37 (m, 8H), 3.21 (m, 8H, CH₂).

Bu₄P[Cp*W₆O₁₈], 4b. 94% yield. IR (ν , cm^{-1}): 991s, 960s, 890s 800s. Anal. Calc. for $\text{C}_{26}\text{H}_{51}\text{O}_{18}\text{PW}_6$: C, 17.5; H, 2.9. Found: C, 19.6; H, 2.8. TGA: formal loss of Cp* and 4 Bu; % exp. (calcd): 20.0 (20.3). ^1H NMR ($\text{DMSO-}d_6$): δ 0.95 (q, 12H, Me), 1.46 (m, 8H, CH₂), 1.59 (m, 8H, CH₂), 2.13-2.28 (m, 8H, CH₂) 2.40 (s, 15H, Cp*). ^{31}P NMR ($\text{DMSO-}d_6$): δ 35.1.

Ph₄P[Cp*W₆O₁₈], 4c. 77% yield. IR (ν , cm^{-1}) 990sh, 960s, 890s, 803s. Anal. Calc. for $\text{C}_{34}\text{H}_{35}\text{O}_{18}\text{PW}_6$: C, 21.9; H, 1.9. Found: C, 23.1; H, 1.7. TGA: loss of Ph₄PCp*; % exp.

(calcd): 26.5 (25.4). ¹H NMR (DMSO-*d*₆): δ 2.4 (s, 15H, Cp*), 7.6-8.1 (m, 15H, Ar). ³¹P NMR (DMSO-*d*₆): δ 23.6. MS: *m/z* = 1525.3 (theor. 1524.7), [Cp*W₆O₁₈]⁻.

X-ray analyses. A single crystal of each compound was mounted under inert perfluoropolyether at the tip of glass fibre and cooled in the cryostream of a Bruker APEXII CCD diffractometer for **2a** or an Agilent Technologies XCALIBUR CCD diffractometer for **1c** and **2c**. Data were collected using the monochromatic MoK α radiation (λ = 0.71073). The structures were solved by direct methods (SIR97)⁶⁴ and refined by least-squares procedures on F^2 using SHELXL-97.⁶⁵ All H atoms attached to carbon were introduced in calculation in idealised positions and treated as riding models. The drawing of the molecules was realised with the help of ORTEP32.^{66,67} Crystal data and refinement parameters are shown in Table 4. Crystallographic data (excluding structure factors) have been deposited with the Cambridge Crystallographic Data Centre as supplementary publication no. CCDC 866670 – 866672. Copies of the data can be obtained free of charge on application to the Director, CCDC, 12 Union Road, Cambridge CB2 1EZ, UK (fax: (+44) 1223-336-033; e-mail: deposit@ccdc.cam.ac.uk).

Table 4. Crystal data and structure refinement for all compounds.

Compound	1c ·(CH ₃) ₂ CO	2a	2c ·(CH ₃) ₂ CO
Empirical formula	C ₃₇ H ₄₁ Mo ₆ O ₁₉ P	C ₂₆ H ₅₁ Mo ₅ N O ₁₈ W	C ₃₇ H ₄₁ WMo ₅ O ₁₈ P
Formula weight	1396.31	1329.23	1484.22
Crystal system	Orthorhombic	Monoclinic	Orthorhombic
Space group	<i>Pnma</i>	<i>P2_{1/n}</i>	<i>Pnma</i>
a, Å	14.8994(7)	11.8997(5)	14.9089(5)
b, Å	13.8507(7)	25.9172(13)	13.8674(5)
c, Å	21.2967(8)	12.7160(6)	21.3702(8)
α =	90	90	90
β =	90	90.405(5)°	90
γ =	90	90°	90
Volume, Å ³	4394.9(3)	3921.6(3)	4418.2(3)
Z	4	4	4

D (calcd), Mg/m ³	2.110	2.251	2.231
Abs. coeff., mm ⁻¹	1.773	4.543	4.081
F(000)	2728	2568	2856
Crystal size, mm ³	0.51 x 0.19 x 0.15	0.22 x 0.09 x 0.04	0.43 x 0.08 x 0.03
Theta range, °	2.90 to 26.37	2.82 to 26.02°.	2.89 to 26.37
Reflts collected	24229	21362	24032
Unique reflts [R(int)]	4682 (0.0233)	7429 [R(int) = 0.0773]	4709 (0.0574)
Completeness, %	99.8	96.0 %	99.9
Abs. correction	Multi-scan	Multi-scan	Multi-scan
Max. / min. abs.	1.00000 and 0.722	0.8392 and 0.4348	1.00000 and 0.620
Data / restr. / param.	4682 / 0 / 310	7429 / 0 / 445	4709 / 0 / 310
GOF on F ²	1.138	1.067	0.976
R, wR ² [I>2σ(I)]	0.0271, 0.0621	0.0572, 0.1260	0.0332, 0.0733
R, wR ² (all data)	0.0355, 0.0674	0.0935, 0.1367	0.0543, 0.0809
Resid. density, e.Å ⁻³	0.591 and -0.944	3.134 and -2.442	1.571 and -1.554

Computational Details. The guess geometries for **I** and **II** were based on the crystallographically determined structures of **1a** and **2a**, replacing all Cp* CH₃ groups by H atoms. From the resulting optimized geometries, starting geometries for **III** and **IV** were generated by changing the metal. All optimizations were carried out on the isolated ions using the Gaussian 03 suite of programs⁶⁸ with the B3LYP functional, which includes the three-parameter gradient-corrected exchange functional of Becke⁶⁹ and the correlation functional of Lee, Yang, and Parr.^{70,71} The standard 6-31G** basis set was used for the C, H and O atoms, while the CEP-31G* basis set⁷² was adopted for Mo and W. Analytical frequency calculations were also run on the optimized geometries, yielding positive frequencies for all normal modes. The calculated IR spectra shown in Figure 3 were generated from the DFT-generated

frequencies and intensities by applying Lorentzian functions and adjusting the linewidth to best fit the experimental spectra.

Acknowledgments.

We are grateful to the CNRS, to the IUF (Institut Universitaire de France) and to Celal Bayar University (FBE 2010/082) for financial support, and to CINES (Centre Informatique National de l'Enseignement Supérieur) and CICT (Centre Interuniversitaire de Calcul de Toulouse, project CALMIP) for granting free computational time. We also thank the French Embassy in Ankara and the Syndicat Mixte of the “Communauté D’agglomération Castres-Mazamet” for financial support of the Ph.D. thesis of G.T.C.

References

Bibliography

- (1) Schimanke, G.; Martin, M.; Kunert, J.; Vogel, H. *Z. Anorg. Allg. Chem.* **2005**, *631*, 1289-1296.
- (2) Landau, M. V.; Vradman, L.; Wolfson, A.; Rao, P. M.; Herskowitz, M. *C. R. Chim.* **2005**, *8*, 679-691.
- (3) Mestl, G. *Top. Catal.* **2006**, *38*, 69-82.
- (4) Kampe, P.; Giebeler, L.; Samuelis, D.; Kunert, J.; Drochner, A.; Haass, F.; Adams, A. H.; Ott, J.; Endres, S.; Schimanke, G.; Buhmester, T.; Martin, M.; Fuess, H.; Vogel, H. *Phys. Chem. Chem. Phys.* **2007**, *9*, 3577-3589.
- (5) Endres, S.; Kampe, P.; Kunert, J.; Drochner, A.; Vogel, H. *Appl. Catal. A* **2007**, *325*, 237-243.
- (6) Goddard, W. A.; Chenoweth, K.; Pudar, S.; Van Duin, A. C. T.; Cheng, M. J. *Top. Catal.* **2008**, *50*, 2-18.
- (7) Shiju, N. R.; Gulians, V. V. *Appl. Catal. A* **2009**, *356*, 1-17.
- (8) Baeck, S. H.; Jaramillo, T. F.; Jeong, D. H.; Mcfarland, E. W. *Chem. Commun.* **2004**, 390-391.
- (9) Kunert, J.; Drochner, A.; Ott, J.; Vogel, H.; Fuess, H. *Appl. Catal. A* **2004**, *269*, 53-61.
- (10) Veith, M.; Mathur, S.; Huch, V. *Inorg. Chem.* **1996**, *35*, 7295-7303.
- (11) Veith, M.; Mathur, S.; Huch, V. *J. Am. Chem. Soc.* **1996**, *118*, 903-904.
- (12) Veith, M.; Mathur, S.; Huch, V. *Chem. Commun.* **1997**, 2197-2198.
- (13) Veith, M.; Mathur, S.; Mathur, C.; Huch, V. *Organometallics* **1998**, *17*, 1044-1051.
- (14) Hemmer, E.; Huch, V.; Adlung, M.; Wickleder, C.; Mathur, S. *Eur. J. Inorg. Chem.* **2011**, 2148-2157.
- (15) Kessler, V. G. *Chem. Commun.* **2003**, 1213-1222.
- (16) Kustov, A. L.; Kessler, V. G.; Romanovsky, B. V.; Seisenbaeva, G. A.; Drobot, D. V.; Shcheglov, P. A. *J. Mol. Catal. A* **2004**, *216*, 101-106.
- (17) Pol, S. V.; Pol, V. G.; Kessler, V. G.; Seisenbaeva, G. A.; Solovyov, L. A.; Gedanken, A. *Inorg. Chem.* **2005**, *44*, 9938-9945.
- (18) Werndrup, P.; Seisenbaeva, G. A.; Westin, G.; Persson, I.; Kessler, V. G. *Eur. J. Inorg. Chem.* **2006**, 1413-1422.
- (19) Pope, M. T. *Heteropoly and isopolyoxometalates*; Springer-Verlag: Berlin, 1983.
- (20) Masure, D.; Chaquin, P.; Louis, C.; Che, M.; Fournier, M. *J. Catal.* **1989**, *119*, 415-425.
- (21) Mizuno, N. *Trends Phys. Chem.* **1994**, *4*, 349-362.
- (22) Kim, T.; Burrows, A.; Kiely, C. J.; Wachs, I. E. *J. Catal.* **2007**, *246*, 370-381.
- (23) Gouzerh, P.; Proust, A. *Chem. Rev.* **1998**, *98*, 77-111.
- (24) Proust, A.; Thouvenot, R.; Gouzerh, P. *Chem. Commun.* **2008**, 1837-1852.
- (25) Knoth, W. H. *J. Am. Chem. Soc.* **1979**, *101*, 759-760.
- (26) Knoth, W. H. *J. Am. Chem. Soc.* **1979**, *101*, 2211-2213.

- (27) Zonnevijlle, F.; Pope, M. T. *J. Am. Chem. Soc.* **1979**, *101*, 2731-2732.
- (28) Ammari, N.; Herve, G.; Thouvenot, R. *New Journal of Chemistry* **1991**, *15*, 607-608.
- (29) Judeinstein, P.; Deprun, C.; Nadjo, L. *J. Chem. Soc., Dalton Trans.* **1991**, 1991-1997.
- (30) Mazeaud, A.; Ammari, N.; Robert, F.; Thouvenot, R. *Angew. Chem. Engl.* **1996**, *35*, 1961-1964.
- (31) Oshihara, K.; Nakamura, Y.; Sakuma, M.; Ueda, W. *Catal. Today* **2001**, *71*, 153-159.
- (32) Agustin, D.; Coelho, C.; Mazeaud, A.; Herson, P.; Proust, A.; Thouvenot, R. *Z. Anorg. Allg. Chem.* **2004**, *630*, 2049-2053.
- (33) Agustin, D.; Dallery, J.; Coelho, C.; Proust, A.; Thouvenot, R. *J. Organomet. Chem.* **2007**, *692*, 746-754.
- (34) Li, J.; Huth, I.; Chamoreau, L. M.; Hasenknopf, B.; Lacote, E.; Thorimbert, S.; Malacria, M. *Angew. Chem. Engl.* **2009**, *48*, 2035-2038.
- (35) Dolbecq, A.; Secheresse, F. *Advances in Inorganic Chemistry, Vol 53* **2002**, *53*, 1-40.
- (36) Hayashi, Y.; Toriumi, K.; Isobe, K. *J. Am. Chem. Soc.* **1988**, *110*, 3666-3668.
- (37) Suss-Fink, G.; Plasseraud, L.; Ferrand, V.; Stoeckli-Evans, H. *Chem. Commun.* **1997**, 1657-1658.
- (38) Blenkiron, P.; Carty, A. J.; Peng, S. M.; Lee, G. H.; Su, C. J.; Shiu, C. W.; Chi, Y. *Organometallics* **1997**, *16*, 519-521.
- (39) Shiu, C. W.; Chi, Y.; Carty, A. J.; Peng, S. M.; Lee, G. H. *Organometallics* **1997**, *16*, 5368-5371.
- (40) Suss-Fink, G.; Plasseraud, L.; Ferrand, V.; Stanislas, S.; Neels, A.; Stoeckli-Evans, H.; Henry, M.; Laurency, G.; Roulet, R. *Polyhedron* **1998**, *17*, 2817-2827.
- (41) Artero, V.; Proust, A.; Herson, P.; Gouzerh, P. *Chem. Eur. J.* **2001**, *7*, 3901-3910.
- (42) Artero, V.; Proust, A.; Herson, P.; Thouvenot, R.; Gouzerh, P. *Chem. Commun.* **2000**, 883-884.
- (43) Collange, E.; Garcia, J.; Poli, R. *New J. Chem.* **2002**, *26*, 1249-1256.
- (44) Collange, E.; Metteau, L.; Richard, P.; Poli, R. *Polyhedron* **2004**, *23*, 2605-2610.
- (45) Taban-Çaliskan, G.; Agustin, D.; Demirhan, F.; Vendier, L.; Poli, R. *Eur. J. Inorg. Chem.* **2009**, 5219-5226.
- (46) Fuchs, J.; Jahr, K. F. *Z. Naturforsch., B: Chem. Sci.* **1968**, *23*, 1380.
- (47) Allcock, H.; Bissell, E.; Shawl, E. *Inorg. Chem.* **1973**, *12*, 2963-2968.
- (48) Garner, C.; Howlader, N.; Mcphail, A.; Miller, R.; Onan, K.; Mabbs, F. *J. Chem. Soc., Dalton Trans.* **1978**, 1978, 1582-1589.
- (49) Bottomley, F.; Chen, J. *Organometallics* **1992**, *11*, 3404-3411.
- (50) Proust, A.; Thouvenot, R.; Herson, P. *J. Chem. Soc., Dalton Trans.* **1999**, 51-55.
- (51) Jee, J.-E.; Comas-Vives, A.; Dinoi, C.; Ujaque, G.; Van Eldik, R.; Lledós, A.; Poli, R. *Inorg. Chem* **2007**, *46*, 4103-4113.
- (52) Sözen-Aktaş, P.; Rosal, I. D.; Manoury, E.; Demirhan, F.; Lledós, A.; Poli, R. **in preparation**.
- (53) Fuchs, J.; Freiwald, W.; Hartl, H. *Acta Crystallographica Section B-Structural Science* **1978**, *34*, 1764-1770.
- (54) Che, T. M.; Day, V. W.; Francesconi, L. C.; Fredrich, M. F.; Klemperer, W. G.; Shum, W. *Inorg. Chem.* **1985**, *24*, 4055-4062.
- (55) Mohs, T. R.; Yap, G. P. A.; Rheingold, A. L.; Maatta, E. A. *Inorg. Chem.* **1995**, *34*, 9-10.

- (56) Strong, J. B.; Yap, G. P. A.; Ostrander, R.; Liable-Sands, L. M.; Rheingold, A. L.; Thouvenot, R.; Gouzerh, P.; Maatta, E. A. *J. Am. Chem. Soc.* **2000**, *122*, 639-649.
- (57) Strukan, N.; Cindric, M.; Devcic, M.; Giester, G.; Kamenar, B. *Acta Cryst. C* **2000**, *56*, E278-E279.
- (58) Chatterjee, T.; Sarma, M.; Das, S. K. *Crystal Growth & Design* **2010**, *10*, 3149-3163.
- (59) Huang, W. L.; Todaro, L.; Francesconi, L. C.; Polenova, T. *J. Am. Chem. Soc.* **2003**, *125*, 5928-5938.
- (60) Rocchiccioli-Deltcheff, C.; Thouvenot, R.; Fouassier, M. *Inorg. Chem.* **1982**, *21*, 30-35.
- (61) Rocchiccioli-Deltcheff, C.; Fournier, M.; Franck, R.; Thouvenot, R. *J. Mol. Struct.* **1984**, *114*, 49-56.
- (62) Bridgeman, A. J.; Cavigliasso, G. *Chem. Phys.* **2002**, *279*, 143-159.
- (63) Dinoi, C.; Taban, G.; Sözen, P.; Demirhan, F.; Daran, J.-C.; Poli, R. *J. Organomet. Chem.* **2007**, *692*, 3743-3749.
- (64) Altomare, A.; Burla, M.; Camalli, M.; Cascarano, G.; Giacovazzo, C.; Guagliardi, A.; Moliterni, A.; Polidori, G.; Spagna, R. *J. Appl. Cryst.* **1999**, *32*, 115-119.
- (65) Sheldrick, G. M. *Acta Cryst. A* **2008**, *64*, 112-122.
- (66) Burnett, M. N.; Johnson, C. K. *ORTEP III, Report ORNL-6895*. ; Oak Ridge National Laboratory: Oak Ridge, Tennessee, U.S. , 1996.
- (67) Farrugia, L. J. *J. Appl. Crystallogr.* **1997**, *30*, 565.
- (68) Frisch, M. J.; Trucks, G. W.; Schlegel, H. B.; Scuseria, G. E.; Robb, M. A.; Cheeseman, J. R.; Montgomery, J., J. A.; Vreven, T.; Kudin, K. N.; Burant, J. C.; Millam, J. M.; Iyengar, S. S.; Tomasi, J.; Barone, V.; Mennucci, B.; Cossi, M.; Scalmani, G.; Rega, N.; Petersson, G. A.; Nakatsuji, H.; Hada, M.; Ehara, M.; Toyota, K.; Fukuda, R.; Hasegawa, J.; Ishida, M.; Nakajima, T.; Honda, Y.; Kitao, O.; Nakai, H.; Klene, M.; Li, X.; Knox, J. E.; Hratchian, H. P.; Cross, J. B.; Adamo, C.; Jaramillo, J.; Gomperts, R.; Stratmann, R. E.; Yazyev, O.; Austin, A. J.; Cammi, R.; Pomelli, C.; Ochterski, J. W.; Ayala, P. Y.; Morokuma, K.; Voth, G. A.; Salvador, P.; Dannenberg, J. J.; Zakrzewski, V. G.; Dapprich, S.; Daniels, A. D.; Strain, M. C.; Farkas, O.; Malick, D. K.; Rabuck, A. D.; Raghavachari, K.; Foresman, J. B.; Ortiz, J. V.; Cui, Q.; Baboul, A. G.; Clifford, S.; Cioslowski, J.; Stefanov, B. B.; Liu, G.; Liashenko, A.; Piskorz, P.; Komaromi, I.; Martin, R. L.; Fox, D. J.; Keith, T.; Al-Laham, M. A.; Peng, C. Y.; Nanayakkara, A.; Challacombe, M.; Gill, P. M. W.; Johnson, B.; Chen, W.; Wong, M. W.; Gonzalez, C.; Pople, J. A. *Gaussian 03, Revision D.01*; Gaussian, Inc.: Wallingford CT, 2004.
- (69) Becke, A. D. *J. Chem. Phys.* **1993**, *98*, 5648-5652.
- (70) Lee, C. T.; Yang, W. T.; Parr, R. G. *Phys. Rev. B* **1988**, *37*, 785-789.
- (71) Miehlich, B.; Savin, A.; Stoll, H.; Preuss, H. *Chem. Phys. Lett.* **1989**, *157*, 200-206.
- (72) Stevens, W. J.; Krauss, M.; Basch, H.; Jasien, P. G. *Canad. J. Chem.* **1992**, *70*, 612-630.

Table of Content Text and Graphic

“Self-assembly” of the $\{\text{Cp}^*\text{M}\}^{5+}$ ($\text{M}' = \text{Mo}, \text{W}$) fragment, derived from $\text{Cp}^*\text{M}_2\text{O}_5$, and molybdate or tungstate ions in a 1:5 ratio in acidic aqueous solution selectively affords the Lindqvist-type polyoxometalate ions $[\text{Cp}^*\text{MM}'_5\text{O}_{18}]^-$.

